

	<b>Algorithm Document</b> <b>FRESCO+ for GOME-2</b>	REF : ISSUE : 1.3 DATE : 18.10.2010 PAGE : 1/1
---	--	---

## **Cloud retrieval algorithm for GOME-2:**

### **FRESCO+**

P. Wang, O. Tuinder, P. Stammes (KNMI)

(18 October 2010, version 1.3)

**Eumetsat contract EUM/CO/09/4600000655/RM**

	<p style="text-align: center;"><b>Algorithm Document</b> <b>FRESCO+ for GOME-2</b></p>	<p>REF : ISSUE : 1.3 DATE : 18.10.2010 PAGE : 2/2</p>
---	--	---

## TABLE OF CONTENTS

<b>1. INTRODUCTION .....</b>	<b>3</b>
<b>2. ALGORITHM DESCRIPTION .....</b>	<b>4</b>
2.1 Forward model.....	4
2.2 FRESCO+ snow/ice mode.....	6
2.3 Retrieval method.....	6
2.4 Databases and auxiliary data in FRESCO+ .....	7
2.4.1 <i>Transmission database</i> .....	7
2.4.2 <i>Surface albedo database</i> .....	9
2.4.3 <i>Surface height database</i> .....	10
2.4.4 <i>Spectral wavelength grid</i> .....	10
2.4.5 <i>Atmospheric profile</i> .....	10
2.4.6 <i>Cloud albedo</i> .....	10
<b>3. VALIDATION.....</b>	<b>12</b>
<b>4. CONSTRAINTS, LIMITATIONS AND ASSUMPTIONS.....</b>	<b>14</b>
4.1 Effective cloud fraction .....	14
4.2 Cloud pressure .....	14
4.3 Cloud albedo and pressure over snow/ice .....	14
4.4 Suggestions for application of the FRESCO+ cloud product .....	15
4.5 Known problems and possible solutions .....	15
4.5.1 <i>Surface albedo database</i> .....	15
4.5.2 <i>Snow/ice detection</i> .....	15
4.5.3 <i>Sun glint over ocean</i> .....	16
4.6 Additional suggestions for users of the FRESCO+ software.....	16
4.7 Range for FRESCO+ input and output parameters and exceptions .....	16
<b>5. REFERENCES .....</b>	<b>18</b>
<b>6. APPENDIX .....</b>	<b>21</b>
6.1 Rayleigh scattering cross section and phase function .....	21
6.2 Atmospheric optical thickness and transmission.....	22
6.3 Single Rayleigh scattering reflectance .....	23

	<p style="text-align: center;"><b>Algorithm Document</b> <b>FRESCO+ for GOME-2</b></p>	<p>REF : ISSUE : 1.3 DATE : 18.10.2010 PAGE : 3/3</p>
---	--	---

## 1. INTRODUCTION

Clouds strongly affect the trace gas retrievals by shielding, albedo enhancement and in-cloud absorptions. Because of the relatively coarse spatial resolution of the GOME-2 satellite instrument ( $40 \times 80 \text{ km}^2$ ), only 5-15% of the pixels are cloud-free (Krijger et al., 2007). To be able to use the majority of GOME-2 pixels, cloud correction is necessary. To correct for cloud effects on trace gas retrievals, the most relevant cloud parameters are the cloud fraction and height (Koelemeijer and Stammes, 1999, Stammes et al., 2008). There are several cloud retrieval algorithms that have been developed for GOME and SCIAMACHY using the  $\text{O}_2 A$  band (Koelemeijer et al., 2001, Kokhanovsky et al., 2005, van Diedenhoven et al., 2007) or using Polarisation Monitoring Devices (PMDs) (Grzegorski et al., 2006, Loyola et al. 2004). FRESCO (Koelemeijer et al., 2001) is a simple, fast and robust algorithm, which is also implemented in the GOME-2 level 1 data processor at EUMETSAT (Munro and Eisinger, 2004, Fournier et al., 2004; Wang and Stammes, 2007).

It is almost impossible to derive uniquely both cloud fraction and cloud optical thickness from the measured spectral reflectance of a single GOME-2 pixel. This is because cloudy scenes with the same cloud pressure may possess different cloud fractions and cloud optical thicknesses, which give rise to nearly the same reflectance in and around the oxygen  $A$  band. For cloudy scenes differing in this sense, however, cloud effects on the ozone column density retrieval are almost the same. Therefore, it is useful and necessary to introduce an effective cloud fraction, which is the cloud fraction derived from the satellite measurements, assuming an a priori chosen cloud optical thickness or cloud albedo. Then, the most relevant cloud parameters for trace gas column density retrieval reduce to effective cloud fraction and cloud pressure. Alternatively, separation of cloud fraction and cloud optical thickness could be done using PMD information, although ambiguity remains to some extent in that approach too.

The FRESCO method was originally developed for near real time ozone column retrieval from GOME (Piters et al., 1999). In Koelemeijer et al. (2001), the FRESCO method is described together with a sensitivity study and validation using ATSR-2 data. In Koelemeijer et al., (2002), a comparison is made between cloud pressures and effective cloud fractions of FRESCO and ISCCP on a monthly average basis. FRESCO+ is a new version of the FRESCO algorithm, in which single Rayleigh scattering is added in the reflectance database and the retrieval (Wang et al., 2008). Rayleigh scattering is mainly important for the almost cloud free part of the pixels. The FRESCO+ cloud pressure is more reliable than FRESCO for less cloudy scenes, say for effective cloud fractions  $< 0.15$ . The FRESCO+ improvement is more relevant for tropospheric trace gas retrievals (like  $\text{NO}_2$ ) than for total  $\text{O}_3$  retrieval.

In this document a description of the FRESCO+ algorithm for GOME-2 (=FRESCO v5) is given and several improvements are described.

	<b>Algorithm Document</b> <b>FRESCO+ for GOME-2</b>	REF : ISSUE : 1.3 DATE : 18.10.2010 PAGE : 4/4
---	--	---

## 2. ALGORITHM DESCRIPTION

### 2.1 Forward model

Information on cloud pressure and effective cloud fraction is derived from the reflectivity  $R$  in and around the  $O_2 A$  band. The reflectivity is given by

$$R(\lambda) = \frac{\pi I(\lambda)}{\mu_0 E_0(\lambda)}, \quad (1)$$

where  $I$  is the Earth's reflected radiance ( $\text{W m}^{-2} \text{nm}^{-1} \text{sr}^{-1}$ ) measured by GOME-2,  $E_0$  the incident solar irradiance at the top of the atmosphere through a horizontal surface unit ( $\text{W m}^{-2} \text{nm}^{-1}$ ) measured by GOME-2, and  $\mu_0$  the cosine of the solar zenith angle. Due to instrument temperature variations in orbit, the wavelength grid of the radiances and irradiances may be different for different measurements. Therefore, to calculate the reflectivity, the measurements of  $I(\lambda)$  and  $E_0(\lambda)$  are interpolated to a common grid, the so-called reference wavelength grid, which is also used in the simulations.

To simulate the reflectance spectrum of a partly cloudy pixel inside and outside the  $O_2 A$  band, a simple atmospheric transmission model is used, in which the atmosphere above the ground surface (for the clear part of the pixel) or cloud (for the cloudy part of the pixel) is treated as an absorbing (due to oxygen) and purely Rayleigh scattering medium. Reflection occurs only at the surface or cloud top. The surface is assumed to be Lambertian; the cloud is assumed to reflect either Lambertian or with a BRDF based on Doubling-Adding and Mie calculations. The principle of the FRESCO+ algorithm is shown in Fig. 1 and 2. The reflectivity  $R_{sim}(\lambda; \theta; \theta_0; \varphi - \varphi_0)$  at a wavelength  $\lambda$ , viewing zenith angle  $\theta$ , solar zenith angle  $\theta_0$ , and relative azimuth angle  $\varphi - \varphi_0$  is then given by

$$R_{sim}(\lambda, \theta, \theta_0, \varphi - \varphi_0) = cT_c A_c + (1 - c)T_s A_s + cR_c + (1 - c)R_s, \quad (2)$$

where  $c$  is the effective cloud fraction,  $A_s$  is the surface albedo, and  $A_c$  the cloud albedo.  $T(\lambda, z, \theta, \theta_0)$  is the direct atmospheric transmittance for light entering the atmosphere from the solar direction, propagating down to a level with cloud height  $z_c$  or surface height  $z_s$ , and then propagating to the top of the atmosphere in the direction of the satellite. The absorption and single Rayleigh scattering are taken into account in the light paths for  $T$ .  $R_c(\lambda, z_c, \theta, \theta_0, \varphi - \varphi_0)$  and  $R_s(\lambda, z_s, \theta, \theta_0, \varphi - \varphi_0)$  are the single Rayleigh scattering reflectances due to cloud and surface, respectively.  $\varphi - \varphi_0$  is the relative azimuth angle of the observation w.r.t. the sun. The sign of

$\varphi - \varphi_0$  is not important because cosine of  $\varphi - \varphi_0$  is used to calculate the scattering angle and sunglint deviation angle (see Eqs. 8 and 11). The transmission and reflectance are calculated using line-by-line calculations through the entire  $O_2$  A band and convoluted with the instrumental response function. To speed up the algorithm the transmissions and single Rayleigh scattering reflectances are pre-calculated and stored in look-up-tables.  $A_s$  and  $z_s$  are taken from a surface albedo database and a surface height database, respectively.  $A_c$  is assumed to be 0.8 or the reflectance at 758 nm if the reflectance is larger than 0.8.

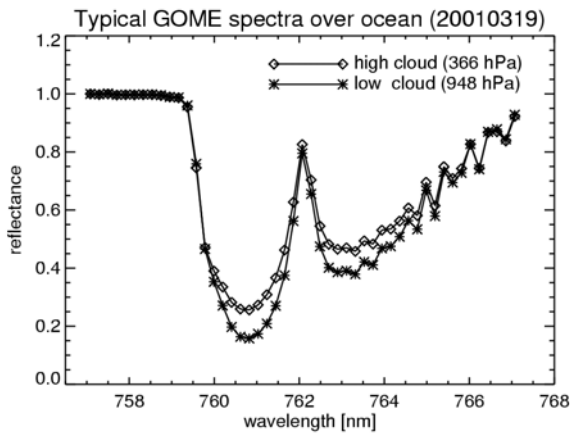


Figure 1. Typical  $O_2$  A-band spectra measured by GOME. The spectra are normalized at 758 nm to show the relative depth of the band for clouds at different heights.

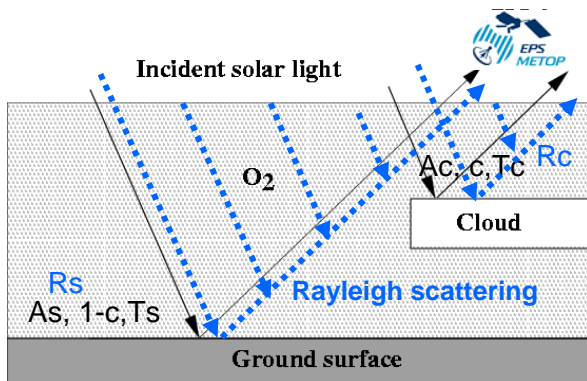


Figure 2. Atmospheric radiation model used in FRESCO+. The cloud and surface are both assumed to be Lambertian reflectors. Three light paths are considered: (1) from sun to surface to satellite, (2) from sun to cloud to satellite, (3) from sun to atmosphere to satellite according to single Rayleigh scattering (indicated in blue). Along all three paths  $O_2$  absorption and Rayleigh scattering are included in the forward model simulations.

	<b>Algorithm Document</b> <b>FRESCO+ for GOME-2</b>	REF : ISSUE : 1.3 DATE : 18.10.2010 PAGE : 6/6
---	--	---

## 2.2 FRESCO+ snow/ice mode

It can easily be shown that the derived effective cloud fraction becomes very sensitive to errors in  $A_s$  when  $A_s$  approaches  $A_c$ , which may occur for surfaces covered by snow. Hence, in that case it is almost impossible to accurately derive an effective cloud fraction and hence cloud pressure. Therefore, in snow/ice cases we assume  $c=1$ , and the measurements are fitted to the function (cf. Eq. 2):

$$R_{sim}(\lambda, \theta, \theta_0) = T_c(\lambda, z, \theta, \theta_0)A_c + R_c(\lambda, z, \theta, \theta_0, \varphi - \varphi_0). \quad (3)$$

The fit is solving for  $A_c$  and  $z$ , which are the albedo and height of the “lower reflecting boundary” (surface or cloud) of the atmosphere.

Presently, information on snow coverage is obtained from the global database of UV surface LER values, which was derived by Herman and Celarier (1997) from 14.5 years of Total Ozone Mapping Spectrometer (TOMS) data at 340 and 380 nm. According to their database, snow-free land and ocean have surface LER values in the UV smaller than  $\sim 0.2$ .

## 2.3 Retrieval method

The retrieval method is based on minimizing the difference between a measured and a simulated spectrum, using the Levenberg-Marquart nonlinear least-squares method,

$$\chi^2 = \sum_{i=1}^N \left[ \frac{R_{meas}(\lambda_i) - R_{sim}(\lambda_i)}{\varepsilon(\lambda_i)} \right]^2, \quad (4)$$

where  $\varepsilon = \varepsilon_{meas} + \varepsilon_{sim}$  is the sum of the measurement and simulation errors, respectively. The simulation error is fixed on an estimated 1 percent. The summation is over the measurement points used by FRESCO+ in the wavelength interval between 758 and 766 nm, which comprises  $N=15$  wavelengths. The free parameters in the fit are the effective cloud fraction and cloud height. The errors are calculated as the square root of the diagonal elements of the covariance matrix. The cloud pressure error is determined as  $\Delta P = \max(|P_c - P(z_c - \Delta z)|, |P_c - P(z_c + \Delta z)|)$ , with  $\Delta z$  the error in cloud height.

The subroutine used is MRQMIN from Numerical Recipes (Press et al., 1986).

	<b>Algorithm Document</b> <b>FRESCO+ for GOME-2</b>	REF : ISSUE : 1.3 DATE : 18.10.2010 PAGE : 7/7
---	--	---

## 2.4 Databases and auxiliary data in FRESCO+

### 2.4.1 Transmission database

The transmission database has two look up tables now: one is the transmission database due to the oxygen absorption and single Rayleigh scattering, the other one includes the single Rayleigh scattering reflectance database except for the Rayleigh scattering phase function. The Rayleigh scattering phase function is calculated in the retrieval model directly. The transmission calculations are performed in two steps. In the transmission ( $T$ ) and reflectance ( $R$ ) calculations the effect of the Earth's sphericity is taken into account. Temperature and pressure profiles were assumed for a mid-latitude summer atmosphere (Anderson et al., 1986). The  $O_2$  absorptions are calculated with a line-by-line method using HITRAN 2004. The transmission databases are calculated at 1 pm spectral resolution and convoluted with the instrumental slit function.

The depth of the oxygen  $A$  band depends on the absorption optical thickness, above the cloud, which is linear in cloud pressure. However, for practical reasons, the height  $z$  is used rather than the pressure  $P$  as the height variable in the model simulations and retrieval. Since the pressure-height relation in the model is generally different than in the real atmosphere, the retrieved cloud height is converted back to cloud pressure using the same atmospheric profile as was used in the simulations to yield the correct cloud pressure. In FRESCO+, a polynomial expansion is used to describe the height dependence of the transmission  $T$ , and the single Rayleigh scattering reflectance  $R_1$ , (except for the Rayleigh scattering phase function):

$$T(\lambda, z, \theta, \theta_0) = \sum_{i=1}^N \alpha_i(\lambda, \theta, \theta_0) z^i, \quad (5)$$

$$R_1(\lambda, z, \theta, \theta_0) = \sum_{i=1}^N \beta_i(\lambda, \theta, \theta_0) z^i \quad (6)$$

where  $N = 4$  was chosen to give negligible interpolation errors. The advantages of this approach are that (1) the simulation database can be much smaller, and (2) the derivative of the reflectance with respect to height can be obtained analytically (useful for Levenberg-Marquart fitting). Therefore, in the LUTs,  $T$  and  $R$  are represented by  $\alpha_i$  and  $\beta_i$  ( $i = 1, 4$ ), respectively, as a function of solar zenith angle (SZA), viewing zenith angle (VZA), and wavelength. The altitude grid for  $z$  is 0.5 km from 0 to 15 km.

The Rayleigh scattering phase function (without polarization) is calculated using Eqs. 7 and 8:

$$F_R(\Theta) = \frac{3(1 - \rho_n)}{4(1 + \rho_n/2)} \left( \cos^2 \Theta + \frac{1 + \rho_n}{1 - \rho_n} \right). \quad (7)$$

	<b>Algorithm Document</b> <b>FRESCO+ for GOME-2</b>	REF : ISSUE : 1.3 DATE : 18.10.2010 PAGE : 8/8
---	--	---

Here  $\rho_n$  is the depolarization factor, at 750 nm  $\rho_n = 0.02786$ , and  $\Theta$  is the scattering angle:

$$\cos \Theta = -\cos \theta \cos \theta_0 + \sin \theta \sin \theta_0 \cos(\varphi - \varphi_0), \quad (8)$$

where  $\theta$  is the viewing zenith angle,  $\theta_0$  is the solar zenith angle,  $\varphi$  is the viewing azimuth angle, and  $\varphi_0$  is the solar azimuth angle. The definitions of  $\theta$ ,  $\theta_0$ ,  $\varphi - \varphi_0$  are illustrated in Figure 3.  $\Theta$  is shown in Figure A.1. Single Rayleigh scattering reflectance is given by Eq. 9:

$$R_R(\lambda, z_r, \theta, \theta_0, \varphi - \varphi_0) = \frac{F_R(\theta, \theta_0, \varphi - \varphi_0)}{4 \cos \theta_0} \int_{z_r}^{\infty} k_{sca}(\lambda, z) T(\lambda, z, \theta, \theta_0) S_{sp}(\theta, z) dz. \quad (9)$$

The FRESCO+ reflectance LUT consists of  $R_I$ :

$$R_I(\lambda, z_r, \theta, \theta_0) = \int_{z_r}^{\infty} k_{sca}(\lambda, z) T(\lambda, z, \theta, \theta_0) S_{sp}(\theta, z) dz. \quad (10)$$

The advantage of using Eq. 10 is that the azimuth is not needed in the reflectance LUT, which reduces the size of the LUT; the FRESCO+ reflectance LUT has the same parameters as the FRESCO+ transmission LUT. The factor  $\frac{F_R(\theta, \theta_0, \varphi - \varphi_0)}{4 \cos \theta_0}$  is calculated online in the FRESCO+ retrieval program according to the actual geometry angles. More formulas about single Rayleigh scattering are given in the Appendix (Sect. 6) and Wang et al. (2008).

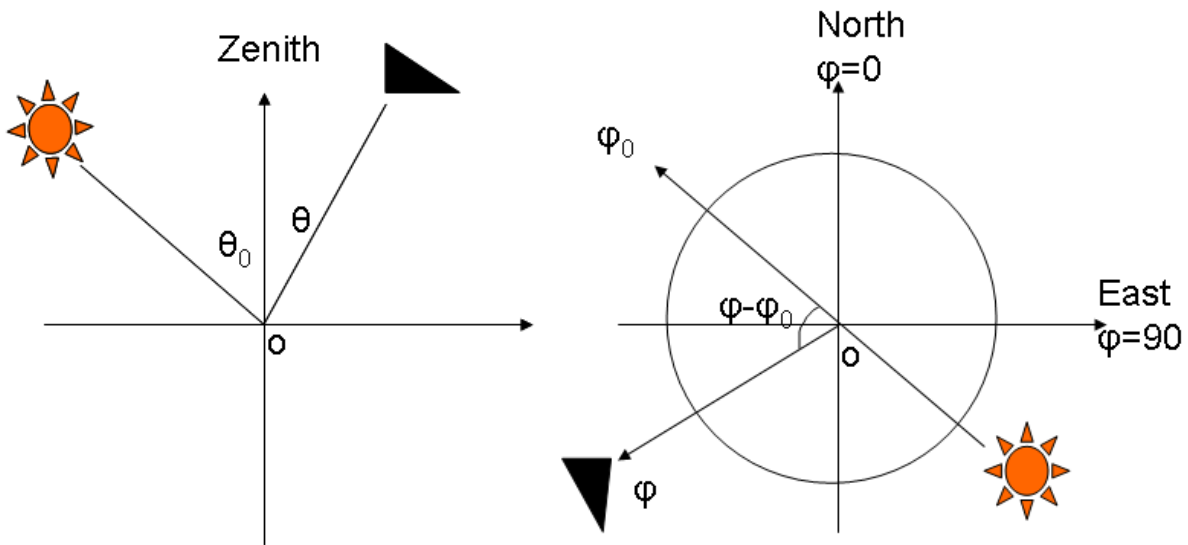


Figure 3. Definitions of solar zenith angle ( $\theta_0$ ), viewing zenith angle ( $\theta$ ) and relative azimuth angle ( $\varphi - \varphi_0$ ) in FRESCO+. In this example  $\varphi_0$  is 315 degree,  $\varphi$  is about 240 degree. The sign of ( $\varphi - \varphi_0$ ) does not matter. The triangle denotes the satellite.

	<b>Algorithm Document</b> <b>FRESCO+ for GOME-2</b>	REF : ISSUE : 1.3 DATE : 18.10.2010 PAGE : 9/9
---	--	---

The definition of the angles could be checked with the sunglint deviation angle  $\Delta\Omega_{gl\text{int}}$  because the sunglint could only appear for the pixels at the right side of the swath when the deviation angles are smaller than 18 degree.  $\Delta\Omega_{gl\text{int}}$  is calculated using Eq. 11.

$$\cos\Delta\Omega_{gl\text{int}} = \cos\theta\cos\theta_0 + \sin\theta\sin\theta_0\cos(\varphi - \varphi_0). \quad (11)$$

If the definition of the relative azimuth angle is wrong, the calculated sunglint position would be at the left side of the swath. The sunglint can be easily identified from the FRESCO+ cloud fraction images.

Currently, in FRESCO+, three about 1-nm-wide wavelength windows are used, namely, 758-759 nm (continuum, no absorption), 760-761 nm (strong absorption), and 765-766 nm (moderate absorption). Each window comprises five GOME-2 wavelengths. It is important to note that the reflectances in these three wavelength windows contain nearly all independent information that is available in the O<sub>2</sub> A band for instruments with the spectral resolution of GOME-2. The detailed information about the transmission database and the tools to create the transmission database for GOME-2 is in the ‘GOME-2 FRESCO final report’ (Wang and Stammes, 2007).

## 2.4.2 Surface albedo database

### 2.4.2.1 GOME LER surface albedo

The surface albedo is deduced from a global surface Lambert-equivalent reflectivity (LER) database that was generated from GOME data of June 1995 - December 2000 (Koelemeijer et al., 2003). This database was generated as follows. For each GOME measurement the LER was determined, using the Doubling-Adding KNMI radiative transfer code (De Haan et al., 1987; Stammes, 2001). The LER is the calculated Lambertian surface albedo required to match the observed reflectance at the top of the atmosphere, assuming a Rayleigh scattering atmosphere. The LERs were binned by month and in grid-cells of 1 deg x 1 deg. The LER of the surface was then determined as the minimum LER in each grid-cell and each month. Effects of persistent clouds over ocean were corrected by replacing the values in such grid-cells by a weighted average of adjacent grid-cells. The GOME albedo climatology was generated for every month for several wavelengths, including 758 and 772 nm used by FRESCO+.

The data is decontaminated from the presence of desert dust aerosols using the GOME Absorbing Aerosol Index (Fournier et al., 2006). The surface albedo is refined at coastlines and made at 0.25°x0.25° resolution (Fournier et al., 2004; Wang and Stammes, 2007).

	<b>Algorithm Document</b> <b>FRESCO+ for GOME-2</b>	REF : ISSUE : 1.3 DATE : 18.10.2010 PAGE : 10/10
---	--	---

GOME surface albedo is the  $A_s$  in Eq. 1 used in the retrieval. The spectral dependence of the surface LER is taken into account by linearly interpolating between the surface LER values at 758 and 772 nm.

#### 2.4.2.2 TOMS surface albedo for detection of snow/ice

The TOMS surface albedo (Herman and Celarier, 1997) is used to identify the presence of snow/ice at the surface for every pixel. Snow/ice coverage is assumed for a GOME-2 pixel if the TOMS database for that area and month gives a UV LER exceeding 0.2, and also when the LER at 758 nm is equal to or larger than the assumed cloud albedo.

#### 2.4.3 Surface height database

The surface height is taken from the GTOPO30 database (made by the U.S. Geological Survey's EROS Data Center in Sioux Falls, South Dakota), downgraded to  $0.25^\circ \times 0.25^\circ$  resolution.

References: data at <http://edcdaac.usgs.gov/gtopo30/gtopo30.asp>  
Documentation at <http://edcdaac.usgs.gov/gtopo30/README.asp>

#### 2.4.4 Spectral wavelength grid

The LUTs for transmission and reflectance are made at a pre-defined wavelength grid. Therefore the spectral wavelength grid is also an auxiliary data set.

#### 2.4.5 Atmospheric profile

The pressure-height relationship in the retrieval model and look-up tables is generally different than in the real atmosphere. Therefore, the retrieved cloud height is converted back to cloud pressure using the same atmospheric profile as was used in the simulations to yield the correct cloud pressure. The standard atmospheric profile for FRESCO+ is the mid-latitude summer profile (Anderson et al., 1986).

#### 2.4.6 Cloud albedo

The cloud albedo is fixed to 0.8. However, when the measured reflectance outside the oxygen  $A$  band (at 758 nm) exceeds this value, the measured reflectance outside the band is used as cloud albedo.

It is also possible to use a BRDF cloud albedo based on Doubling-Adding and Mie calculations. The results are similar as albedo of 0.8 (Koelemeijer et al., 2001). Therefore, a Lambertian cloud albedo is the standard setting in FRESCO+.

	<b>Algorithm Document</b> <b>FRESCO+ for GOME-2</b>	REF : ISSUE : 1.3 DATE : 18.10.2010 PAGE : 11/11
---	--	---

It is important to stress that the effective cloud fraction derived using FRESCO thus pertains to an optically thick cloud: the cloud optical thickness that pertains to a cloud spherical albedo of 0.8 is  $\sim 33$ . The choice for a cloud albedo of 0.8 is based on several considerations. First, the choice  $A_c=0.8$  is optimized for ozone air mass factor calculations in the UV, when a ghost-column is added to the derived vertical column density to correct for ozone below the cloud. Second, in the FRESCO method we assume that absorption below the cloud may be neglected, which can be justified for optically thick clouds. Choosing a high cloud albedo ensures that the model assumptions are internally consistent. More detailed discussion about effective cloud fraction is in the paper by Stammes et al. (2008).

	<b>Algorithm Document</b> <b>FRESKO+ for GOME-2</b>	REF : ISSUE : 1.3 DATE : 18.10.2010 PAGE : 12/12
---	--	---

### 3. VALIDATION

The FRESKO (v4) and FRESKO+ (FRESKO v5) cloud heights have been compared for SCIAMACHY with active remotely sensed cloud heights at the SGP/ARM site. The ARM cloud layer height distributions and the collocated SCIAMACHY FRESKO+ cloud heights are shown in Figure 4. In this plot we have further limited the FRESKO+ effective cloud fractions to values larger than 0.2 and the time periods of ARM cloud cover to periods longer than 30 minutes, which corresponds to geometric cloud fractions larger than 0.5. As shown in Figure 4(a), the FRESKO+ cloud height is close to the middle of the ARM cloud profiles. This agrees with the results of FRESKO+ for simulated spectra. As shown in Figure 4(b), the FRESKO+ cloud heights have an excellent correlation with the averaged ARM cloud profiles, with a correlation coefficient of 0.94. To demonstrate the improvement in FRESKO+, SCIAMACHY FRESKO and ARM cloud heights are shown in Figure 4(c, d). The criteria used for the selection of SCIAMACHY FRESKO and ARM data are similar as that for FRESKO+ and ARM, except that FRESKO effective cloud fractions are larger than 0.2. The different number of data in FRESKO and FRESKO+ is due to the different FRESKO and FRESKO+ effective cloud fractions. As shown in Figure 4(a, c) FRESKO+ retrieves lower cloud height than FRESKO, which agrees with the simulations and the statistics from GOME data. FRESKO+ significantly improves the cloud height retrievals for single-layer low clouds. In this case, FRESKO often does not converge and retrieves a cloud height close to the initial value of 5 km. The correlation coefficient of FRESKO and ARM cloud height is 0.79 (Wang et al., 2008).

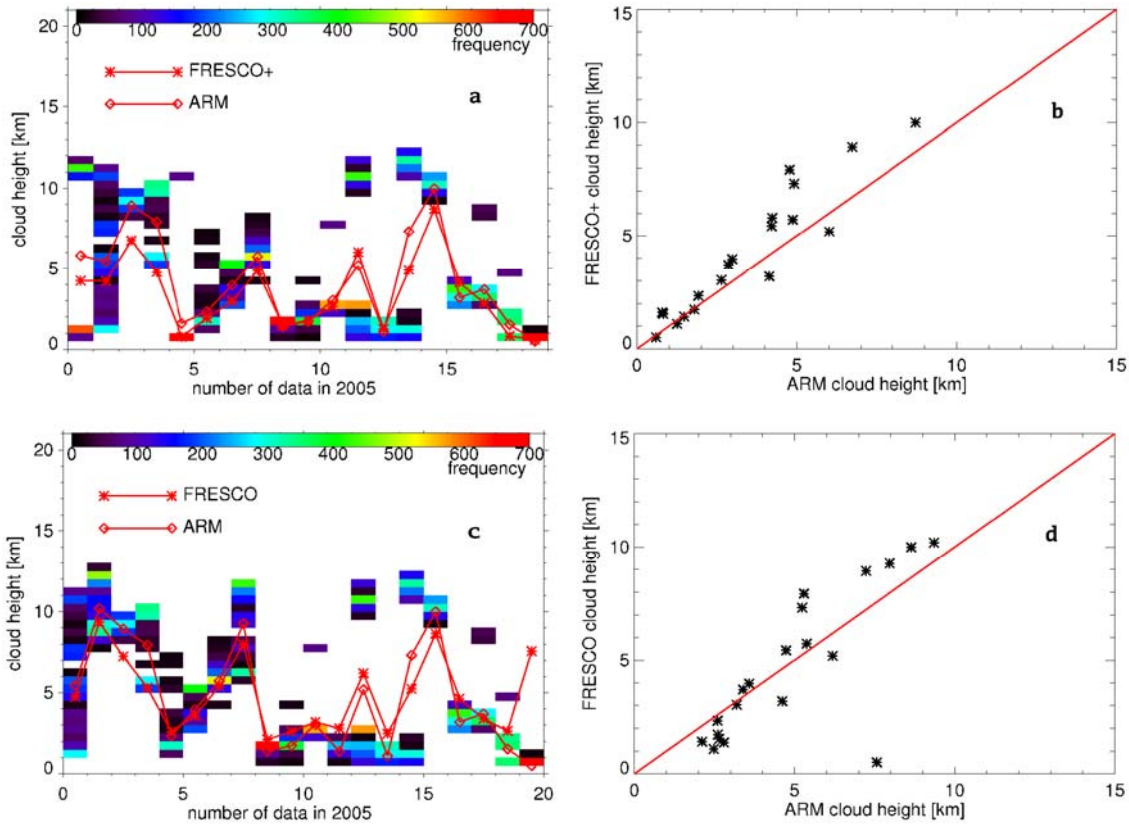


Figure 4. (a) Comparison between collocated SCIAMACHY FRESKO+ cloud heights and ground-based radar/lidar cloud profiles, for 18 days in 2005 on which SCIAMACHY overpasses of the SGP/ARM site occurred. The color indicates the occurrence of clouds as detected by the radar/lidar. (b) Correlation of FRESKO+ cloud height and the average cloud height from the radar/lidar profiles for the same data as in (a), with correlation coefficient of 0.94. (c) and (d) are similar as (a) and (b) but FRESKO data are used. The correlation coefficient between ARM and FRESKO cloud height is 0.79. Only effective cloud fractions larger than 0.2 are used.

	<p style="text-align: center;"><b>Algorithm Document</b> <b>FRESCO+ for GOME-2</b></p>	<p>REF : ISSUE : 1.3 DATE : 18.10.2010 PAGE : 14/14</p>
---	--	---

## 4. CONSTRAINTS, LIMITATIONS AND ASSUMPTIONS

### 4.1 Effective cloud fraction

The FRESCO+ effective cloud fraction is smaller than the geometric cloud fraction, because a Lambertian cloud albedo of 0.8 is used. This means that the effective cloud fraction is a radiometric cloud fraction for an optically thick cloud. The effective cloud fraction would become larger than 1 if the cloud in the pixel is brighter than 0.8. In this case the FRESCO+ cloud fraction is set to 1, and the cloud albedo is adjusted. The effective cloud fraction can have a small negative value ( $> -0.05$ ) from the Levenberg-Marquart fitting. This can happen for cloud-free scenes when the surface albedo from the database is higher than the actual surface albedo. In the fit the cloud fraction is allowed to be between -0.05 and 1.1 to make the fit converge. Because the simple cloud model and the surface albedo database can not be the same as the reality, we need some range for cloud fraction to reduce the numerical problem. The change of cloud fraction leads to a cloud pressure difference of less than 20 hPa, however we cannot tell which pressure is more accurate. In the FRESCO+ output we set the small negative values to 0; this clipping is indicated by the value  $c=0.00000$  as a proxy-flag.  $C_{eff}$  values  $> 1$  are not clipped, since this is useful information; users can clip it themselves. The FRESCO+ cloud fraction range in output is therefore  $[0, 1.1]$ .

### 4.2 Cloud pressure

FRESCO+ uses a Lambertian cloud model, with no scattering inside and below the clouds. Therefore the cloud pressure in FRESCO+ is not the cloud top pressure. From the validation and comparison with DAK model simulations for scattering clouds we find: (1) FRESCO+ cloud height is lower than the cloud top height measured by Lidar/Radar or infrared passive satellite sensors such as MODIS. This has been found from validation with MODIS and Lidar/Radar measurements at the SGP/ARM site. (2) From DAK model simulations using scattering clouds we find that the FRESCO+ cloud height is close to the middle of the cloud or to the optical center of two-layer cloud systems. We note that FRESCO+ cloud height does not distinguish multi-layer clouds.

The FRESCO+ output cloud pressure range is  $[130.0, 1013.0]$  hPa. Cloud pressure is always lower than surface pressure and higher than the pressure level of 15 km, because the altitude range for the LUTs is  $[0, 15]$  km. Cloud pressures which are retrieved outside this range are clipped. The cloud pressure values 130.00000 and 1013.00000 hPa are proxy-flags to indicate clipping.

### 4.3 Cloud albedo and pressure over snow/ice

	<b>Algorithm Document</b> <b>FRESKO+ for GOME-2</b>	REF : ISSUE : 1.3 DATE : 18.10.2010 PAGE : 15/15
---	--	---

In the snow/ice mode, FRESKO+ retrieve cloud albedo and cloud pressure. Actually these are scene albedo and scene pressure because FRESKO+ cannot separate between clouds and surface in this case. The scene albedo and pressure are parameters to be used in the air mass factor calculations for the trace gas retrievals. We do not recommend using the cloud albedo and pressure over snow/ice for other purposes.

The retrieved cloud albedo in snow/ice mode should not be confused with the cloud albedo of 0.8. Especially for very bright scenes the scene albedo can have values  $> 0.8$ .

#### 4.4 Suggestions for application of the FRESKO+ cloud product

The FRESKO+ product is optimal for cloud correction in trace gas retrieval under the same Lambertian cloud assumption. This means that if one uses the FRESKO+ product as a cloud parameter in radiative transfer modelling for trace gas air mass factor (AMF) calculations, the cloud in the AMF calculations should be a Lambertian cloud, which will give the smallest error for the trace gas retrieval. We do not recommend to use FRESKO+ cloud fraction or cloud height directly if one assumes the cloud is a scattering media in the RTM model.

The FRESKO+ product can be used for determining cloud trends and variations on global or regional scales, using monthly averages.

#### 4.5 Known problems and possible solutions

##### 4.5.1 Surface albedo database

The surface albedo database derived from GOME (320 km x 80 km pixel size) is too coarse for SCIAMACHY and GOME-2. Therefore, some bright surface features such as mountains, hills in the Sahara desert show up in the global monthly mean maps of effective cloud fraction from SCIAMACHY. The same features will occur for GOME-2. The effect is not significant globally. However, one has to be careful with the effective cloud fraction data over bright surfaces, like deserts, where the surface albedo might be an issue.

A solution would be to make a new surface albedo database from GOME-2 itself. There is a sufficient amount of data (about 3 years) to make such a database.

##### 4.5.2 Snow/ice detection

Snow/ice is detected according to the TOMS surface albedo climatology (if  $A_s \geq 0.2$  at 360 nm) or if  $A_s \geq 0.8$  at 772 nm in the GOME albedo database. Therefore, FRESKO+ cannot detect

	<b>Algorithm Document</b> <b>FRESCO+ for GOME-2</b>	REF : ISSUE : 1.3 DATE : 18.10.2010 PAGE : 16/16
---	--	---

snow/ice changes on a daily basis, especially at the places with lots of sea ice. The resolution of TOMS surface albedo database is also too coarse ( $1^\circ \times 1^\circ$ ).

It is unlikely that snow coverage is assumed whereas in reality the scene is free of snow. On the other hand, it may occur that in reality snow coverage is present where no snow coverage is assumed. In that case, reflection by the surface is disguised by reflection by a low-level cloud layer. However, for the purpose of ozone column correction, this should have the same effect.

The solution could be to use other instruments on Metop for detecting snow/ice (AVHRR) or using the NISE snow/ice database for snow/ice detection.

#### 4.5.3 Sun glint over ocean

FRESCO+ does not separate sun glint and real clouds. Therefore in the GOME-2 effective cloud fraction maps one can see the sun glint pattern in the eastern side of the swath. In trace gas retrievals the sun glint has a similar effect as clouds, namely an albedo effect. This can be corrected in the same way as clouds are corrected. It appears from FRESCO+ retrievals that the effective cloud fraction of sun glint is around 0.2, with a cloud pressure at surface pressure.

### 4.6 Additional suggestions for users of the FRESCO+ software

The previous sections were mainly focussed on the FRESCO+ principle and products. To implement the FRESCO+ software the following points have to be considered.

- 1) The FRESCO+ software does not have subroutines to read GOME-2 L1 data. Therefore the solar irradiance, earth radiance and the corresponding errors have to be provided as input.
- 2) The definition of relative azimuth angle can be different for different instruments. It can be checked by the calculation of sun glint position. For GOME-2 the sun glint should be at the east side of the swath over ocean, as can be seen from the effective cloud fraction maps. If the relative azimuth is wrong, the calculated sun glint position would be at west side of the pixels. The relative azimuth for the correct sun glint position is the correct one. The definition of the angles for GOME-2 is in the document "GOME-2 Level 1 product Generation Specification (EUMETSAT 2006)".

### 4.7 Range for FRESCO+ input and output parameters and exceptions

	Parameters	Value or range	Comments
	max. number of iterations in Levenberg Marquart	10	Usually 5 is enough

	<b>Algorithm Document</b> <b>FRESCO+ for GOME-2</b>	REF : ISSUE : 1.3 DATE : 18.10.2010 PAGE : 17/17
---	--	---

input	fit		
	Lambertian cloud albedo (not used if MIE_C1 is used)	0.800	In the code, Ac is reset to refl(1) if refl(1) > 0.8
	UV albedo threshold for snow/ice mode	0.200	Detect snow/ice (as360.ge.uvalb).or.(as758.ge.cldalb)
	minimum surface albedo 758--772 nm	0.010	if (as758.lt.asmin) as758=asmin if (as772.lt.asmin) as772=asmin
	first-guess effective cloud fraction	0.500	
	first-guess cloud top height [km]	5.000	
	first-guess cloud albedo	0.500	
	chi-square variation cut-off value	1.000e-5	
	error in simulated reflectivity (errsim)	1.000e-2	Absolute error, the value can affect the fit especially when the fit is not good. sig(i) = errrefl(i) + errsim
	maximum allowed solar zenith angle	89.5	
	maximum allowed measured reflectivity	4.5	If only nadir viewing, 1.5 is better
output	Effective cloud fraction	[0, 1.1]	In the fit, the allowed range is Ceff = [-0.05, 1.1]. In the output, Ceff=0.00000 indicates clipping of negative Ceff values. Ceff values larger than 1 are not clipped, since this is useful information. Users can clip the Ceff>1 values to 1.0000.
	Cloud pressure	[surface pressure, 130 hPa]	Converted from cloud height [km] using fix atmospheric profile. Clipping of values > 1013 hPa: pc = 1013.00000 hPa Clipping of values < 130 hPa: pc = 130.00000 hPa.
	Cloud height (optional output)	[surface height, 15 km]	LUT is made up to 15 km
	Cloud albedo (for snow/ice mode)	[0, 1]	
In the code	Errors of earthshine spectrum and irradiance spectrum	Read from L1 data	Absolute errors. erad, errerad: earthshine spectrum and the error. Sirr, errsirr: Solar irradiance spectrum and the error
	Error of reflectance (errrefl)		errrefl(i)=refl(i)*sqrt((errerad(i)/erad(i))**2+(errsirr(i)/sirr(i))**2)
	SZA, VZA, AZI	[28,89.5], [0,70], [0,180]	Values are defined at surface level. Definitions see Fig. 4 (in appendix).
	Surface albedo	Surface albedo database	If (as758.gt.refl(1)) as758=refl(1) as772=refl(1)

	<b>Algorithm Document</b> <b>FRESCO+ for GOME-2</b>	REF : ISSUE : 1.3 DATE : 18.10.2010 PAGE : 18/18
---	--	---

## 5. REFERENCES

Anderson, G. P., S. A. Clough, F. X. Kneizys, J. H. Chetwynd, and E. P. Shettle, AFGL atmospheric constituent profiles, Tech. Rep. AFGL-TR-86-0110, Air Force Geophys. Lab., Hanscom AFB, Mass., 1986.

Bates, D. R., Rayleigh scattering by air, *Planet. Space Sci.*, Vol. 32, No. 6, pp. 785-790, 1984.

Clothiaux, E. E., T. P. Ackerman, G. G. Mace, K. P. Moran, R. T. Marchand, M. A. Miller, and B. E. Martner, Objective determination of cloud heights and radar reflectivities using a combination of active remote sensors at the ARM CART sites, *J. Appl. Meteorol.*, 39, 645– 665, 2000.

van Diedenhoven B., O. P. Hasekamp, J. Landgraf (2007), Retrieval of cloud parameters from satellite-based reflectance measurements in the ultraviolet and the oxygen A-band, *J. Geophys. Res.*, 112, D15208, doi:10.1029/2006JD008155.

Fournier, N., P. Stammes, J.R. Acarreta, J. van Geffen, FRESCO Cloud Algorithm for GOME-2, Final Report, ESTEC contract number 17332/03/NL/GS, 2004.

Fournier, N., P. Stammes, M. de Graaf, R. van der A, A. Pitters, M. Grzegorski, A. Kokhanovsky, "Improving cloud information over deserts from SCIAMACHY Oxygen A-band measurements", *Atmos. Chem. Phys.*, 6, 163-172, 2006, <http://www.copernicus.org/EGU/acp/acp/6/163/acp-6-163.htm>

Grzegorski, M., M. Wenig, U. Platt, P. Stammes, N. Fournier, T. Wagner, 2006, The Heidelberg iterative cloud retrieval utilities (HICRU) and its application to GOME data, *ACPD* 1679-1723, SRef-ID: 1680-7375/acpd/2006-6-1679.

De Haan, J. F., P. B. Bosma, and J. W. Hovenier, The adding method for multiple scattering calculations of polarized light, *Astron. Astrophys.*, 183, 371-391, 1987.

Herman, J. R. and E. A. Celarier, Earth surface reflectivity climatology at 340-380 nm from TOMS data, *J. Geophys. Res.*, 102, 28,003-28,011, 1997.

Hovenier, J. W., Domke, H., van der Mee, C., *Transfer of Polarized Light in Planetary Atmospheres: Basic Concepts and Practical Methods*, Kluwer academic publishers, Dordrecht/Boston/London, 2005.

Koelemeijer, R. B. A., and P. Stammes, Effects of clouds on ozone column retrieval from GOME UV measurements, *J. Geophys. Res.*, 104, 8281-8294, 1999.

	<b>Algorithm Document</b> <b>FRESCO+ for GOME-2</b>	REF : ISSUE : 1.3 DATE : 18.10.2010 PAGE : 19/19
---	--	---

Koelemeijer, R. B. A., P. Stammes, J. W. Hovenier, and J. F. de Haan, A fast method for retrieval of cloud parameters using oxygen A band measurements from GOME, *J. Geophys. Res.*, 106, 3475-3490, 2001.

Koelemeijer, R. B. A., P. Stammes, J. W. Hovenier, and J. F. de Haan, Global distributions of effective cloud fraction and cloud top pressure derived from oxygen A band spectra measured by the Global Ozone Monitoring Experiment: comparison to ISCCP data, *J. Geophys. Res.*, 107(D12), 4151, doi: 10.1029/2001JD000840, 2002.

Koelemeijer, R. B. A., J.F. de Haan, P. Stammes, A database of spectral surface reflectivity in the range 335-772 nm derived from 5.5 years of GOME observations, *J. Geophys. Res.*, 108(D2), 4070, doi: 10.1029/2002JD002429, 2003.

Kokhanovsky, A.A, V. V. Rozanov, T. Nauss, C. Reudenbach, J. S. Daniel, H. L. Miller, J. P. Burrows, 2005: The semianalytical cloud retrieval algorithm for SCIAMACHY-I. The validation, *Atmos. Chem. Phys. Discuss.*, 5, 1995-2015.

Krijger, J., M. van Weele, I. Aben, and R. Frey (2007), Technical note: The effect of sensor resolution on the number of cloudfree observations from space, *Atmos. Chem. Phys.*, 7, 2881–2891.

Loyola, D.: Automatic Cloud Analysis from Polar-Orbiting Satellites Using Neural Network and Data Fusion Techniques, in: Proceedings of the IEEE International Geoscience and Remote Sensing Symposium, IGARSS'2004, Anchorage, vol. 4, pp. 2530–2534, 2004.

Munro, R. and Eisinger, M., The Second Global Ozone Monitoring Experiment (GOME-2) An Overview, Programme Development Department Technical Memorandum No.11, October 2004.

Piters, A. J. M., P. J. M. Valks, R. B. A. Koelemeijer, and D. M. Stam, GOME ozone fast delivery and value-added products algorithm specification document, Tech. Rep. GOFAP-KNMI-ASD-01, 23 pp., R. Neth. Meteorol. Inst., De Bilt, Netherlands, 1999.

Press, W. H., B. P. Flannery, S. A. Teukolsky, and W. T. Vetterling, *Numerical Recipes*, 818 pp., Cambridge Univ. Press, New York, 1986.

Rothman, L. S., Jacquemart, D., Barbe, A. et al., The HITRAN 2004 molecular spectroscopic database, *Journal of Quantitative Spectroscopy & Radiative Transfer* 96 (2005) 139–204.

Stammes, P., Spectral radiance modelling in the UV-visible range, in: Proceedings of the International Radiation Symposium 2000: Current problems in Atmospheric Radiation, eds. W. L. Smith and Y. M. Timofeyev, A. Deepak Publ., Hampton, 2001.

Stammes, P., Sneepe M., de Haan, J. F., Veeffkind, J. P., Wang, P., and Levelt, P. F.: Effective cloud fractions from OMI: theoretical framework and validation, *J. Geophys. Res.*, 113, D16S38, doi:10.1029/2007JD008820, 2008.

	<b>Algorithm Document</b> <b>FRESCO+ for GOME-2</b>	REF : ISSUE : 1.3 DATE : 18.10.2010 PAGE : 20/20
---	--	---

Tilstra, L. G., N. A. J. Schutgens, P. Stammes, Analytical calculation of stokes parameters Q and U of atmospheric radiation, Koninklijk Nederlands Meteorologisch Instituut (KNMI), De Bilt, The Netherlands, August 2003. Scientific report = Wetenschappelijk Rapport; WR-2003-01, De Bilt, 2003, ISSN : 0169-1651, ISBN : 90-369-2237-2.

Wang, P., P. Stammes, F. Boersma, "Impact of the effective cloud fraction assumption on tropospheric NO<sub>2</sub> retrievals", in: Proceedings of the Atmospheric Science Conference, ESA ESRIN, Frascati, Italy, 8-12 May 2006.

Wang, P., P. Stammes, FRESCO-GOME2 project 'Additions to EPS/MetOp RAO project #3060', EUM/CO/06/1536/FM, final report, 14 September, 2007.

Wang, P., P. Stammes, R. van der A, G. Pinardi en M. van Roozendaal, FRESCO+: an improved O<sub>2</sub> A-band cloud retrieval algorithm for tropospheric trace gas retrievals, *Atm. Chem. Phys.*, 2008, 8, 9697-9729.

	<b>Algorithm Document</b> <b>FRESCO+ for GOME-2</b>	REF : ISSUE : 1.3 DATE : 18.10.2010 PAGE : 21/21
---	--	---

## 6. APPENDIX

In this appendix, the formulae for the FRESCO+ simulations of the O<sub>2</sub> A-band reflectance are given which is an update of the FRESCO formulae given by Koelemeijer et al. (2001).

### 6.1 Rayleigh scattering cross section and phase function

The Rayleigh scattering cross section,  $\sigma_R$ , is calculated with the formula (Bates, 1984):

$$\sigma_R = (32\pi^3 / 3N^2\lambda^4)(n_{air} - 1)^2 F_K'(air), \quad (A.1)$$

where  $(n_{air} - 1)$  is the refractive index, and  $F_K'(air)$  is the effective King correction factor. The effective King correction factors and refractive index for air are chosen at 750 and 800 nm from table 1 in Bates (1984), and are linearly interpolated between 750 and 800 nm.

The Rayleigh scattering phase function (without polarization) is given by,

$$F_R(\Theta) = \frac{3(1 - \rho_n)}{4(1 + \rho_n/2)} \left( \cos^2 \Theta + \frac{1 + \rho_n}{1 - \rho_n} \right), \quad (A.2)$$

$$\cos \Theta = -\cos \theta \cos \theta_0 + \sin \theta \sin \theta_0 \cos(\varphi - \varphi_0), \quad (A.3)$$

where  $\Theta$  is the scattering angle,  $\theta$  is the viewing zenith angle,  $\theta_0$  is the solar zenith angle,  $\varphi$  is the viewing azimuth angle, and  $\varphi_0$  is the solar azimuth angle.  $\rho_n$  is the depolarization factor; at 750 nm  $\rho_n = 0.02786$ .

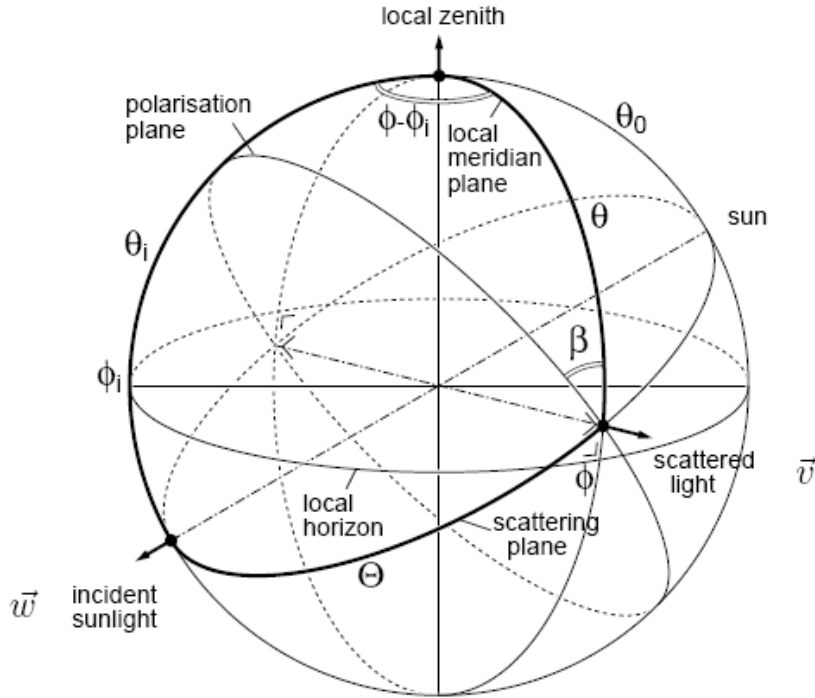


Figure A.1 Definition of the SZA, VZA and AZI in FRESCO+. (Figure is from Tilstra et al., 2003)

## 6.2 Atmospheric optical thickness and transmission

The atmospheric optical thickness and transmission is determined by oxygen absorption and Rayleigh scattering. The absorption is calculated from the number density of  $O_2$  molecules ( $n_{O_2}$ ) and the  $O_2$  absorption cross section,  $\sigma_{O_2}(\lambda, T(z), P(z))$ , along the light path;  $T, P$  are omitted from the notation from this point onwards. The absorption coefficient (in 1/m) is given by:

$$k_{abs}(\lambda, z) = n_{O_2}(z) \sigma_{O_2}(\lambda, z). \quad (A.4)$$

The Rayleigh scattering coefficient is calculated from the air density ( $n_{air}$ ) and the Rayleigh scattering cross section ( $\sigma_R(\lambda, z)$ ),

$$k_{sca}(\lambda, z) = n_{air}(z) \sigma_R(\lambda, z). \quad (A.5)$$

The total atmospheric optical thickness,  $\tau$ , is the sum of the absorption and scattering contributions:

	<b>Algorithm Document</b> <b>FRESCO+ for GOME-2</b>	REF : ISSUE : 1.3 DATE : 18.10.2010 PAGE : 23/23
---	--	---

$$\tau(\lambda, z_r, \theta, \theta_0) = \int_{z_r}^{\infty} (k_{abs}(\lambda, z) + k_{sca}(\lambda, z))(S_{sp}(\theta_0, z - z_r) + S_{sp}(\theta, z - z_r))dz, \quad (\text{A.6})$$

Here:  $S_{sp}(\theta_0, z - z_r)$  and  $S_{sp}(\theta, z - z_r)$  are the spherical light path factors from the sun to the reflector and from the reflector to the satellite (Koelemeijer et al., 2001).  $z$  is height in the atmosphere,  $z_r$  is the altitude of the reflector (surface or clouds).  $\theta_0, \theta$  are the solar zenith angle and viewing zenith angle at surface height.

The transmission from TOA to  $z_r$ , assuming a reflector at altitude  $z_r$ , and back from  $z_r$  to TOA is now given by:

$$T(\lambda, z_r, \theta, \theta_0) = e^{-\tau(\lambda, z_r, \theta, \theta_0)}. \quad (\text{A.7})$$

$T$  is stored in a look-up-table.

### 6.3 Single Rayleigh scattering reflectance

The single Rayleigh scattering reflectance,  $R_R$ , is calculated with the formula (see Fig. 2) (Hovenier et al., 2005),

$$R_R(\lambda, z_r, \mu, \mu_0, \varphi - \varphi_0) = \frac{F_R(\mu, \mu_0, \varphi - \varphi_0)}{4\mu_0\mu} \int_{z_r}^{\infty} k_{sca}(z)T(\lambda, z, \mu, \mu_0)dz, \quad (\text{A.8})$$

where  $T(\lambda, z, \mu, \mu_0)$  is transmission,  $\mu_0 = \cos \theta_0$ ,  $\mu = \cos \theta$ . We have to modify Eq. A.8 for the spherical light path:

$$R_R(\lambda, z_r, \theta, \theta_0, \varphi - \varphi_0) = \frac{F_R(\theta, \theta_0, \varphi - \varphi_0)}{4 \cos \theta_0} \int_{z_r}^{\infty} k_{sca}(\lambda, z)T(\lambda, z, \theta, \theta_0)S_{sp}(\theta, z)dz. \quad (\text{A.9})$$

Since we can neglect the wavelength dependence of the Rayleigh scattering phase function,  $F_R$ , in the O<sub>2</sub> A-band, we can multiply by the phase function in Eq. A.9 after the convolution with the slit function. Therefore the reflectances are stored in a look-up-table (LUT) as:

$$R_1(\lambda, z_r, \theta, \theta_0) = \int_{z_r}^{\infty} k_{sca}(\lambda, z)T(\lambda, z, \theta, \theta_0)S_{sp}(\theta, z)dz. \quad (\text{A.10})$$

Another advantage of using Eq. A.10 is that the azimuth is not needed in the reflectance LUT, which now has the same parameters as the FRESCO+ transmission LUT. The factor

	<b>Algorithm Document</b> <b>FRESCO+ for GOME-2</b>	REF : ISSUE : 1.3 DATE : 18.10.2010 PAGE : 24/24
---	--	---

$\frac{F_R(\theta, \theta_0, \varphi - \varphi_0)}{4 \cos \theta_0}$  is calculated in the FRESCO+ retrieval program according to the measurement geometry.

In the main text  $R_s$  and  $R_c$  are  $R_R$  for clear sky and cloudy cases, respectively.  $R_c = R_R(\lambda, z_c, \theta, \theta_0, \varphi - \varphi_0)$ ,  $R_s = R_R(\lambda, z_s, \theta, \theta_0, \varphi - \varphi_0)$ , where  $z_c$  is the altitude of the cloud, and  $z_s$  is the surface height.